2021 43rd Annual International Conference of the
IEEE Engineering in Medicine & Biology Society (EMBC)
Oct 31 - Nov 4, 2021. Virtual Conference

A Simulation Study on Electrical Activity of Ventricular Endocardial Tissue due to SCN5A L812Q Mutation

Helan Satish and Ramasubba Reddy M, *Member, IEEE*

***Abstract*— Brugada Syndrome is a rare arrhythmia, hereditary in nature. It is caused due to mutation in genes that encodes sodium ion channels and it results sudden cardiac death in young adults. This paper aims to model a two dimensional SCN5A L812Q mutated endocardial tissue by modifying the model equations for sodium ion channel in the Ten Tusscher model for human ventricular tissue. Results show that the propagation of electrical activity in the mutated cells is slower when compared to the normal cells of the endocardial tissue. From this it is concluded that there is a large reduction of sodium current in the mutated region of the endocardial tissue. This leads to reduction in the total ionic current as well and further reduces the membrane potential. It also leads to the slower propagation of action potential in the mutated region when compared to the normal endocardial tissue.**

***Clinical Relevance*— This establishes the propagation of electrical activity in endocardial tissue for SCN5A L812Q gene mutation that results in arrhythmia called Brugada Syndrome.**

I. Introduction

Brugada syndrome is a rare cardiac arrhythmia that is due to loss of function mutation in sodium ion channels. It is a channelopathy and it usually leads to sudden cardiac death in young adults of Asian countries [1]. Antiarrhythmic drugs do not help prolonging the life of the individual. There are many loss of function mutations that leads to arrhythmia. SCN5A L812Q is one among them [2].

This genetic defect causes reduction in amplitude of the sodium current and leads to abnormalities in ECG. As BrS is a rare arrhythmia, experimental study is tough and so there is a need for simulation study. Computational cardiology plays an important role in understanding the mechanisms of cardiac arrhythmia. It helps us to understand changes in the ionic currents, behavior of the channel and ion channel mutations at a sub-cellular, cellular and further to the whole heart.

Effect of loss of function mutation on SCN5A gene due to L812Q mutant in the DII-S4 transmembrane region of the sodium channel protein is studied by considering the steady state activation and inactivation, time constants, sodium ionic current and action potential of the epicardial cell. Reduction in the spike of the action potential due to SCN5A L812Q gene mutation is observed. This reduction in the action potential spike is due to the reduced sodium current inflow [3]. In this paper, a model of homogeneous two dimensional normal endocardial tissue grid was made. To study how the action potential propagates from one cell to the another in the mutated endocardial tissue, SCN5A L812Q gene mutation is introduced in the endocardial tissue grid by modifying the equations of sodium ion channel given by Wang et al. [4]. A mutated region of different size is introduced in the normal endocardial tissue and the behavior of the tissue is analyzed. This is done to show how much delay the mutated tissue introduces in the propagation of action potential when compared to the normal tissue.

II. Materials And Methods

A. Model Characterization

Model of an endocardial cell was made using the biophysical model developed by Ten Tusscher et al. for human ventricular tissue [5]. The following ordinary differential equation (Eq.1) was used to model an endocardial cell.

$$\frac{dV}{dt} = -\frac{I_{ion} + I_{stim}}{C_m} \quad (1)$$

where t is the time, C_m is the membrane capacitance, I_{stim} is the external stimulus current and I_{ion} is the sum of transmembrane currents given below.

$$I_{ion} = I_{Na} + I_{KI} + I_{to} + I_{Kr} + I_{Ks} + I_{CaL} + I_{NaCa} + I_{NaK} + I_{pCa} + I_{pK} + I_{bCa} + I_{bNa} \quad (2)$$

The time dependent gating variables m, h and j for I_{Na}, r and s for I_{to}, xr1 and xr2 for I_{kr}, xs for I_{ks}, d, f, and f_{Ca} for I_{CaL} and g for I_{rel} were solved using Rush and Larson scheme. Other equations were solved using Euler method. In order to simulate the electrophysiological effects of the SCN5A L812Q mutation, the parameters of I_{Na} were modified to incorporate the experimentally observed properties given by Wang et al.[4]. The general equation for sodium current I_{Na} is given below

$$I_{Na} = G_{Na}\, m^3 hj(V\text{-}E_{Na}) \quad (3)$$

where G_{Na} is the sodium conductance, m is the activation gate, h is the fast inactivation gate, j is the slow inactivation gate, V is the resting membrane potential and E_{Na} is the equilibrium potential of sodium ion.

Helan Satish is with the Biomedical Engineering Group, Department of Applied Mechanics, Indian Institute of Technology Madras, Tamil Nadu, India; (e-mail: littleflower.helan@gmail.com).

Ramasubba Reddy M is with the Biomedical Engineering Group, Department of Applied Mechanics, Indian Institute of Technology Madras, Tamil Nadu, India (e-mail: rsreddy@iitm.ac.in).

B. Equations for Normal Cells

The equations for gating variables m, h and j of the activation and inactivation gates for the normal cell is given below [4].

$$m = \frac{1}{[1 + e^{(-40.91-V)/5.10}]} \quad (3)$$

$$h = \frac{1}{[1 + e^{(-72.70-V)/8.00}]} \quad (4)$$

$$j = \frac{1}{[1 + e^{(-72.70-V)/8.00}]} \quad (5)$$

C. Equations for SCN5A L812Q Mutated Cells

The equations m, h and j of the activation and inactivation gates for SCN5A L812Q mutated cell is given below [4].

$$m = \frac{1}{[1 + e^{(-41.24-V)/4.72}]} \quad (6)$$

$$h = \frac{1}{[1 + e^{(-92.40-V)/6.20}]} \quad (7)$$

$$j = \frac{1}{[1 + e^{(-92.40-V)/6.20}]} \quad (8)$$

Other equations such as α_m, β_m, τ_m, α_h, β_h, τ_h , α_j, β_j, τ_j are considered the same as that of the normal cell [5].

D. 2-dimensional model of the tissue

Simulation of an endocardial cell was made by following the Ten Tusscher [5] model and the equations for sodium channels from [4] were used for normal and mutated endocardial cells. MATLAB R2019b was used for the simulation study.

Sodium ion channels play an important role in the development and propagation of electrical activity of cardiac cells. To observe the propagation of electrical activity in an endocardial tissue, a 100x100 cell grid is considered. The cells are interconnected by using gap junction conductance which connects the intracellular spaces of two adjacent myocytes. Propagation of electrical activity from one cell to another of the grid takes place by using the method shown in [6]. Mutated cells of square shaped region were introduced in different sizes to include inhomogeneity in the cell grid to show the relative speed of propagation of action potential in the normal and mutated cells in the tissue.

In general, 2-dimensional model of the tissue is formed by solving the reaction diffusion equation (partial differential equation), however a method of discrete connection of cells is used for the formation of a 2-dimensional endocardial tissue grid for this study. A 3x3 grid using discrete connection of cells is shown in Fig.1 as an example. The same procedure is adapted for the 100x100 grid. This discrete connection of cells has feasibility in varying individual cell parameters such as conductance, membrane potential, changes in initial values, by observing the behavior of specific cells in the tissue, etc. The corner most cells of the array are coupled to 3 adjacent cells, cells at the borders are connected to 5 neighboring cells and the cells in the inner array interact with 8 closest cells. Gap junction conductance helps the passage of ionic current from one cell to another when there exists a difference in membrane potential between the two neighboring cells [6] [7][8].

The flow of current from one cell to another for a cell in this grid is determined by the sum of product of difference in voltage between that cell and its surrounding neighbors and the conductance between them. The current (I_{stim}) to stimulate a cell (i,j) is given as

$$\begin{aligned} I_{stim} &= (V_{i-1,j-1} - V_{i,j})G_{i-1,j-1} + (V_{i-1,j} - V_{i,j})G_{i-1,j} \\ &+ (V_{i-1,j+1} - V_{i,j})G_{i-1,j+1} + (V_{i,j-1} - V_{i,j})G_{i,j-1} \\ &+ (V_{i,j+1} - V_{i,j})G_{i,j+1} + (V_{i+1,j-1} - V_{i,j})G_{i+1,j-1} \\ &+ (V_{i+1,j} - V_{i,j})G_{i+1,j} + (V_{i+1,j+1} - V_{i,j})G_{i+1,j+1} \end{aligned} \quad (9)$$

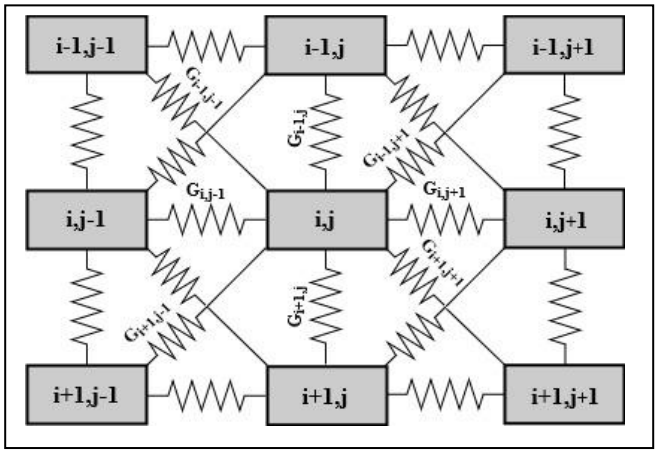

Figure 1. Discrete connection of endocardial cells showing a 3x3 grid

E. Electrical activity in endocardial tissue

The tissue grid used for this study contain 100 columns of cells in which the column on the extreme left is numbered as column 1 and one on the extreme right as column 100. The row at the top of the cell grid is considered as row 1 and one at the bottom is row 100. Uniform gap junction conductance of 0.06 nS is considered between the cells. The study is conducted on normal tissue, mutated tissue and combination of both normal and mutated tissue.

For a normal tissue grid with parallel excitation, the entire first column of the cell grid was excited with a stimulus current of 52 μA for a duration of 1 ms. Gating variables and the corresponding ionic currents are calculated using Eq.1 to 5 at an interval of 0.8 ms. The excitation wavefront propagates parallelly from left to right of the cell grid. Since the uppermost and lowermost cells of each column have smaller number of neighboring cells, propagation takes little more time than all the other cells of the column. In the same fashion, mutated cell grid is formed and excited at the leftmost column of the cell grid. To calculate the gating variables and the corresponding ionic currents Eq.3, 4 and 5 were replaced with Eq. 6, 7 and 8.

Similarly, a combination of normal and mutated cell grid is formed by replacing the normal cells with a square of side 20x20 mutated cells at different locations of the normal cell grid keeping remaining cells of the grid as normal cells. Results for the 20x20 mutated cells embedded in a normal cell grid of 100x100 cells is shown in this paper. Gating variables and the corresponding ionic currents for the normal cells and mutated cells are calculated using appropriate equations from Eq.1 to 8. In another type of excitation, a 2x2 group of cells at the top left corner of the cell grid were excited simultaneously with the stimulus current of 52 μA for a duration of 1 ms. Gating variables and the corresponding

ionic currents for the normal cells, mutated cells and the combination of normal and mutated cell are calculated as above. The excitation wavefront propagates diagonally from top left corner to bottom right corner of the cell grid.

III. Results And Discussions

A. Electrical Activity in Normal Tissue and SCN5A L812Q Mutated Endocardial Tissue.

Fig. 2 shows the parallel propagation of both normal and mutated endocardial tissue in a 100x100 cell grid. The corresponding time taken for the propagation is mentioned on top of each graph. In Fig.1. (a), the cells in the first column take 4 ms to depolarise. Once these cells get depolarised, a potential difference is formed between the cells of column 1 and column 2. These cells of column 1 pass current to those in column 2 to excite them forming a source sink relationship. This results in a depolarisation wavefront that moves from left to right, parallel to columns at the left and right sides of the endocardial tissue grid. Colormap shows the variation in action potential from resting membrane potential to the depolarized potential. Black color represents that the cells are repolarized and yellow color represents that the cells are depolarized. An activation map is also plotted to show the excitation times of each cell in the grid.

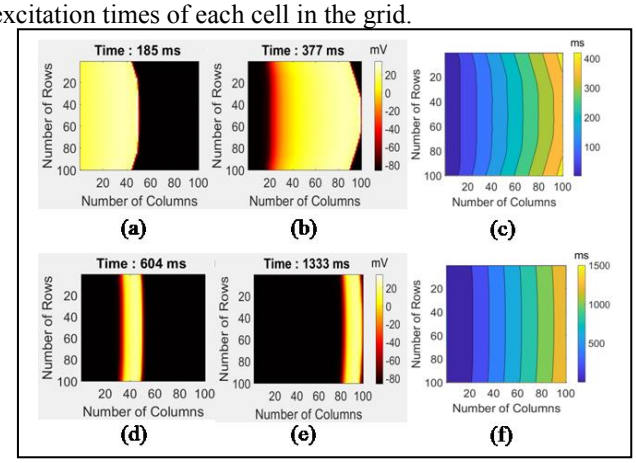

Figure 2. Parallel propagation in normal and mutated endocardial cell grid. (D = Depolarization, PE = Parallel Excitation, AM = Activation Map, Time in millisecond (ms))
(a) D of (50,50) cell of the normal cell grid in PE (b) D of (50,100) cell of the normal cell grid in PE. (c) AM of normal cell grid in PE
(d) D of (50,50) cell of the mutated cell grid in PE (e) D of (50,100) cell of the mutated cell grid in PE. (f) AM of mutated cell grid in PE

From Fig.2 (a) and (b) it can be observed that, depolarization starts from the left side of the tissue and propagates to the right. For the parallel propagation of normal endocardial tissue, depolarization wavefront reaches (50,50) cell at 185 ms and (50,100) cell at 377 ms. For the mutated tissue, the time taken to depolarize the (50,50) cell is 604 ms and (50,100) at 1333 ms as shown in Fig.2 (d) and (e). Slower propagation of action potential in the mutated tissue is observed.

For diagonal excitation, the 2x2 cell group get depolarised in 4 ms and then pass current to their neighbouring cells due to the potential difference between the cells and their neighbours. This results in a wave, propagating diagonally from left top corner to right bottom corner as seen in Fig.3 (a), (b), (d) and (e). The time taken for the action potential to propagate diagonally in a normal endocardial tissue to reach (50,50) cell is 338 ms and it reaches (100,100) cell at 668 ms. For diagonal excitation of mutated tissue, the wavefront reaches (50,50) cell at 1304 ms and (100,100) cell at 2406 ms as plotted in Fig.3 (d) and (e).

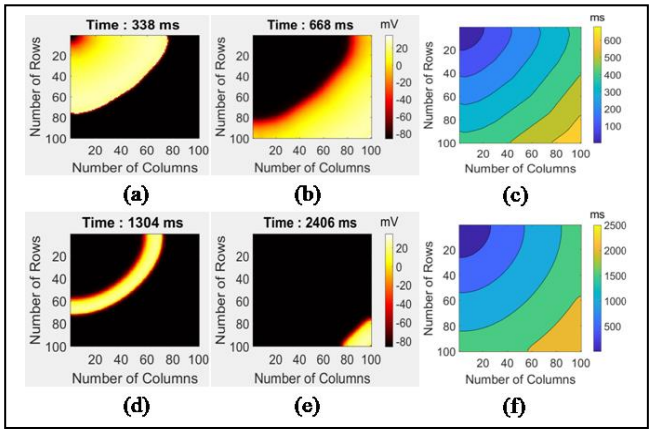

Figure 3. Diagonal propagation in normal and mutated endocardial cell grid. (D = Depolarization, DE= Diagonal Excitation, AM = Activation Map, Time in millisecond (ms))
(a) D of (50,50) cell of the normal cell grid in DE (b) D of (100,100) cell of the normal cell grid in DE. (c) AM of normal cell grid in DE
(d) D of (50,50) cell of the mutated cell grid in DE. (e) D of (100,100) cell of the mutated cell grid in DE. (f) AM of mutated cell grid in DE

B. Propagation of Electrical Activity in the cell grid with combination of normal and SCN5A L812Q Mutated cells.

1) Parallel Propagation

Input stimulus was applied to the entire first column of cells and the movement of action potential was observed. From Fig.4 (a) it is seen that the cells from column 1 starts depolarizing similar to the normal endocardial tissue until it reaches 41st column. Once it reaches the mutated region, propagation becomes slower in the patch region due to the reduction in sodium ion current that leads to smaller I_{ion}.

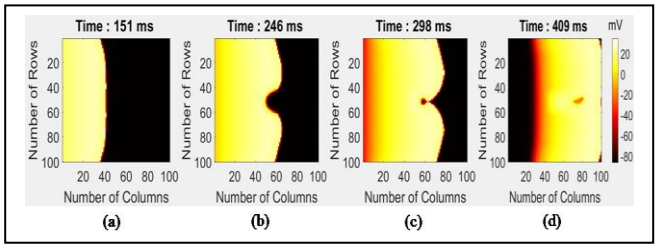

Figure 4. Parallel Excitation (PE) in SCN5A L812Q mutated tissue of 20x20 cells in a 100x100 endocardial tissue. (D = Depolarization, Time in millisecond (ms)) (a) D of the cell (50,41) at 151 ms (Mutated cells in the 41st column) (b) D of the cell (50,50) at 246 ms (c) D of the cell (50,60) at 298 ms (d) D of the cell at (50,100) at 409 ms.

The first column of the cell grid depolarizes at 4 ms. The time taken to depolarize (50,50) cell is 246 ms whereas for a normal cell grid it is 185 ms. Cells above and below the patch of mutated cells propagates similar to the normal endocardial tissue. Action potential propagation in the mutated region is observed slower than the normal endocardial tissue. The excitation wavefront initially goes around the perimeter of the mutated square patch and reaches (50,60) at 298 ms. Finally, it reaches the cell (50,100) at 409 ms. The activation map shown in Fig.6 (a) explains the above mechanism.

2) Diagonal Propagation

Input stimulus was applied to the 2x2 cell grid at the top left corner of the endocardial cell grid and the movement of action potential was observed. From Fig.5 (a) it is seen that the cells from the 2x2 grid starts depolarizing similar to the normal endocardial tissue until it reaches the patch of mutated tissue at (41,41). Once it reaches the mutated region, propagation becomes slower in the patch region due to the reduction in sodium ion current that leads to smaller I_{ion}. The time taken to depolarize (50,50) cell is 397 ms whereas for a normal cell grid it is 338 ms. Cells other than the patch of mutated cells propagates similar to the normal endocardial tissue.

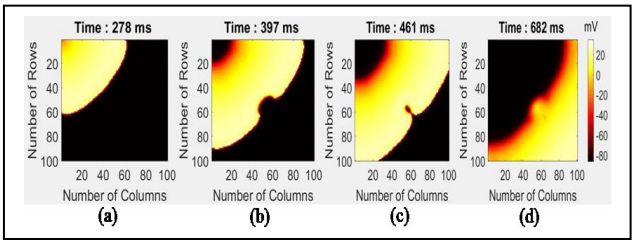

Figure 5. Diagonal Excitation (DE) in SCN5A L812Q mutated issue of 20x20 cells in a 100x100 endocardial tissue. (D = Depolarization, Time in millisecond (ms)) (a) D of the cell (41,41) at 278 ms, (b) D of the cell (50,50) at 397 ms (c) D of the cell (60,60) at 461 ms (d) D of the cell (100,100) at 682 ms.

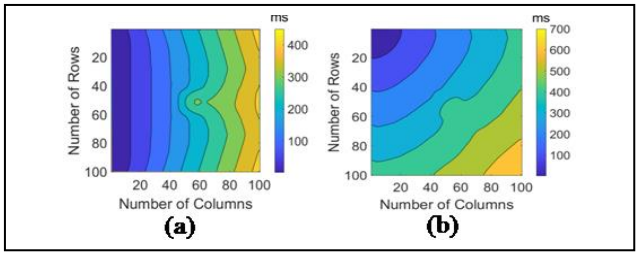

Figure 6. AM for the combination of normal and SCN5A L812Q mutated tissue of 20x20 cells in a 100x100 endocardial tissue. (a) Parallel Excitation (b) Diagonal Excitation

Action potential propagation in the mutated region is observed slower than the normal endocardial tissue. The excitation wavefront initially goes around the perimeter of the mutated square patch and reaches (60,60) at 461 ms. Finally, it reaches the cell (100,100) at 682 ms. The above mechanism can be visualized in the activation map shown in Fig.6 (b).

IV. Conclusion

Brugada Syndrome is a hereditary disease caused due to mutation in genes that encodes sodium ion channel. SCN5A L812Q is one among them. This study was conducted to find the effect of SCN5A L812Q gene mutation in an endocardial tissue. A 100x100 cell grid of normal, mutated and combined normal and mutated endocardial tissue is simulated for parallel and diagonal excitation. It is observed that the propagation of electrical activity is slower in mutated endocardial tissue when compared to the normal endocardial tissue. This delay is due to the reduction in sodium ion current because of the SCN5A L812Q gene mutation. This leads to reduction in total ionic current I_{stim}. Above study was conducted in an endocardial tissue embedded with a patch of mutated tissue of size 10x10 cells, 20x20 cells and other increased sizes placed at different locations of the cell grid keeping all the other cells as normal cells. Slower propagation of electrical activity is observed in both parallel and diagonal propagation in the endocardial tissue with a patch of mutated tissue. It is also found that propagation delay is observed more in larger size of mutated tissue than smaller size. Larger the number of mutated cells, larger the delay in propagation of electrical activity takes place. For a parallel propagation in two dimensional tissue grid of size 100x100 cells with a gap junction conductance of 0.06 nS, the mean conduction velocity is found as 0.32 cells/ms for Ten Tusscher model and 0.26 cells/ms for the model used for this study. Future work includes the investigation of effect of variation in gap junction conductance in the propagation of action potential for a two dimensional tissue.

References

[1] C. Antzelevitch, "Genetic, molecular and cellular mechanisms underlying the J wave syndromes," Circ. J., vol. 76, no. 5, pp. 1054–1065, 2012.

[2] W. Li, L. Yin, C. Shen, K. Hu, J. Ge, and A. Sun, "SCN5A variants: Association with cardiac disorders," Frontiers in Physiology, vol. 9, no. OCT. Frontiers Media S.A., p. 1372, 09-Oct-2018.

[3] H. Satish and R. R. Machireddy, "Computational Study of SCN5A L812Q Gene Mutation in Epicardial Cells," in 2020 IEEE-EMBS Conference on Biomedical Engineering and Sciences (IECBES), 2021, pp. 46–50.

[4] L. Wang et al., "De novo mutation in the SCN5A gene associated with brugada syndrome," Cell. Physiol. Biochem., vol. 36, no. 6, pp. 2250–2262, 2015.

[5] K. H. W. J. Ten Tusscher, D. Noble, P. J. Noble, and A. V. Panfilov, "A model for human ventricular tissue," Am. J. Physiol. - Hear. Circ. Physiol., vol. 286, no. 4 55-4, pp. 1573–1589, 2004.

[6] J. Mayourian, E. A. Sobie, and K. D. Costa, "An introduction to computational modeling of cardiac electrophysiology and arrhythmogenicity," in Methods in Molecular Biology, vol. 1816, Humana Press Inc., 2018, pp. 17–35.

[7] R. Malathi and M. R. S. Reddy, "Effect of Gap Junction Conductance and Formation of Reentry in Human Ventricle Tissue – a Computational Study," no. March, pp. 85–88, 2009.

[8] P. Kirthi Priya and M. R. Reddy, "Study of factors affecting the progression and termination of drug induced Torsade de pointes in two dimensional cardiac tissue," J. Electrocardiol., vol. 50, no. 3, pp. 332–341, May 2017.